A HOLOGRAPHIC INTERFEROMETER SYSTEM FOR MEASURING DENSITY PROFILES IN HIGH-VELOCITY FLOWS

Alpheus W. Burner

NASA Langley Research Center

Hampton, Virginia

ABSTRACT

This paper describes a holographic interferometric technique for obtaining density measurements across a test gas that is traveling at a velocity of over 5500 meters per second in an expansion tube facility. Interferometric data describing the flow in the test section are obtained using a long coherence length cw argon laser in a holographic system and a rotating drum camera recorder. The object beam, which passes through the test section, intersects the reference beam at a small angle (5°) to form an interference pattern of about 170 lines/mm, and is recorded as a hologram. Before a test, this hologram is placed in its original position and rotated slightly so that an interference pattern is generated by the intersection of the reconstructed and real-time object beams. This interference pattern is adjusted to a series of bright, horizontal fringes having a spatial frequency of about 5 fringes/cm. During the few milliseconds it takes the test gas to pass through the test section, variations in the gas density across the 8.4-cm test section produce phase variations in the object beam and result in a varying interference pattern. A rotating drum camera with a 0.15-mm slit alined perpendicular to the fringes is used to record the varying fringe shifts with a time resolution of about 3 microseconds. The average gas density across the test section is determined by measuring these fringe shifts.

INTRODUCTION

Aerodynamic researchers need to have detailed knowledge of flow-field characteristics in order to effectively evaluate new aerodynamic concepts. Qualitative flow analysis is normally obtained using the conventional schlieren and shadowgraph techniques. Quantitative measurements describing the flows are usually obtained with probes. These probes alter the flow significantly where wind-tunnel test sections are relatively small. Ideally, quantitative measurements of the flow density should be obtained without disturbing the flow field. In the past, such density measurements were usually made in high-speed facilities using the Mach-Zehnder interferometer. The application of this technique requires expensive high-quality tunnel windows and optics and the problems of maintaining the system alinement during testing have limited its general use (1).

The development of holography has added a new optical technique, holographic interferometry, for obtaining gas density measurements. The double pulse and dual hologram systems have both been investigated and demonstrated to be effective methods for determining gas density changes (2,3). These techniques use short-duration pulsed lasers which offer the advantage of being able to operate in a vibratory environment, but do not provide the capability to obtain real-time density data required to describe nonsteady flows.

Earlier laboratory studies indicated that real-time holography would be suitable for real-time gas density measurements in a facility with little more setup difficulty than required for a schlieren system (4). In this holographic interferometric technique, a hologram is first recorded with no flow in the test section. After development, this hologram is repositioned so that an interference pattern of convenient spatial frequency and orientation is observed. Any changes in the density in the optical volume will result in fringe shifts caused by changes in the index of refraction.

It is the purpose of this paper to discuss the application of this technique to a facility and give data analysis procedures in which fringe shifts are converted to average density measurements. A detailed analysis of the density data will be presented in a future NASA report by K. James Weilmuenster.

LIST OF SYMBOLS

c	Constant in Lorentz-Lorenz formula
d	Spacing between maxima of interference pattern recorded as hologram
k	Gladstone-Dale constant = 0.226 cm^3/g
ℓ	Width of test section = 8.4 cm
M	Number of wavelengths of optical path length change (fringe shift)

n	Index of refraction in the test section during flow
n_o	Index of refraction initially in the test section
s	Path of the light ray
x	Direction of flow
y	Direction of the vertical test-section height
z	Direction of propagation of light ray
θ	Reference-to-object beam angle = 5°
λ_o	Wavelength outside test section = 5145 Å
ρ	Density in test section during flow
ρ_o	Density initially in test section
$\bar{\rho}$	Average density across test section

THEORY

The intersection of two coherent monochromatic plane waves forms an interference pattern in the region of overlap (Fig. 1). It is this interference pattern which is recorded on a photographic plate as a hologram. If the object beam is perpendicular to the hologram, the spacing between maximas is given by

$$d = \frac{\lambda_o}{\sin \theta}$$

where λ_o is the wavelength of the laser outside the test section and θ is the angle between the reference and object beams (5). After development and repositioning, the hologram acts as a diffraction grating to diffract both the object and reference beams into several orders. If the hologram is placed exactly in its original position, the object beam orders are exactly superimposed on the reference beam orders and no interference pattern is formed. This is similar to the infinite fringe case for a Mach-Zehnder interferometer. In the infinite fringe case, a phase alteration of sufficient magnitude in either the object or reference beams will produce a fringe interference pattern. These fringes are lines of constant phase, and therefore represent lines of constant density since the phase change is proportional to the density change. This type of fringe pattern is difficult to analyze quantitatively since there is generally no reference density from which to determine the density changes (1). For this reason, the hologram is rotated slightly to produce an interference fringe pattern with a convenient spatial frequency of approximately five lines/cm. These fringes are oriented horizontally in the direction of flow (Fig. 2). In this case, the undisturbed fringes are used as a reference and any fringe shift is measured from a time when the density is known (the prerun or undisturbed condition). The fringe shift can then be converted into average density.

In order to facilitate repositioning of the hologram after development, the object-to-reference beam angle θ was kept as small as possible (about 5°). Once the hologram is repositioned and fringes are observable, the desired fringe orientation and spacing is obtained by rotating the plate slightly. For horizontal fringes, the hologram must have a slight rotation about the x axis (direction of flow) (Fig. 2). The hologram was properly oriented before each run with little difficulty.

Since these fringes are interference fringes, the conversion from fringe shift to density can be analyzed in the same manner as for a Mach-Zehnder interferometer. The following treatment applies to both and is presented here for completeness.

The change in optical path length of a light ray passing through the test section resulting from a change in the index of refraction in the test section optical volume can be expressed in terms of wavelength λ_o outside the test section as

$$\int_s [n(s) - n_o]\, ds = M\lambda_o$$

where M is the number of wavelengths, λ_o, of optical path length change, $n(s)$ is the index of refraction in the test section during flow, n_o is the index of refraction initially in the test section, and s is the path of the light ray (6).

If refraction effects are neglected, M can be measured as a fringe shift at a point on the holographically produced interferogram. Rewriting the above equation

$$\int_o^{\ell} [n(x,y,z) - n_o]dz = M(x,y)\lambda_o$$

where ℓ is the width of the test section. The orthogonal coordinates x,y, and z are oriented with x in the direction of flow, z in the direction of the propagation of the object beam, and y in the direction of the vertical test section height (Fig. 2).

The theoretical Lorentz-Lorenz formula (6) relating the density ρ to the index of refraction n,

$$\frac{n^2 - 1}{n^2 + 2} = c\rho$$

where c is a constant, can be rewritten as,

$$\left(\frac{n + 1}{n^2 + 2}\right)(n - 1) \doteq c\rho$$

Since the index of refraction for air is very close to unity for the density range considered, $(n - 1)$ is the dominant term and the $(n+1)/(n^2+2)$

term is essentially a constant. Thus the Lorentz-Lorenz formula may be rewritten as, $n - 1 = k\rho$, which is the experimental Gladstone-Dale formula where k is the Gladstone-Dale constant (1).

Thus the equation relating the optical path length to fringe shift can be rewritten as,

$$\int_0^{\ell} [\rho(x,y,z) - \rho_o]dz = \frac{M(x,y)}{k} \lambda_o$$

where $\rho(x,y,z)$ is the density in the test section during flow and ρ_o is the initial density in the test section.

The x coordinate is fixed by the location of the slit on the test section and the y coordinate is fixed by the point of evaluation on the interferogram. Therefore, for a fixed x,y position, ρ is a function of z only and the above integral equation may be written as,

$$\int_0^{\ell} \rho(x_1,y_1,z)\ dz = \frac{M\lambda_o}{k} + \rho_o\ \ell$$

Dividing through by the width of the test section yields the average density $\overline{\rho}$,

$$\overline{\rho(x_1,y_1)} = \rho_o + \frac{\lambda_o M}{k\ell}$$

Then the average density across the test section at any height can be determined from the magnitude of the fringe shift measured from the reference position at a known density.

SOURCES OF ERROR

Major sources of error in this technique are refraction in high-density gradient regions, density gradients in the optical volume external to the test section, and measurement of the fringe shift from the film record. Refraction is a factor only in regions of high-density gradients such as at a shock normally visible with schlieren or in high-density gradient boundary layers. Density gradients external to the test section can be lessened by simply insuring that no blower, heater, or air conditioner is operating in the vicinity of the setup during a test run. The effect of these gradients can be determined by measuring the fringe shift of the undisturbed fringes for a period of time comparable to the run time.

The largest error results from measuring the fringe shift from the film record. With care, the fringe shift can be measured to within 0.1 fringe shift which corresponds to an average density error of less than $\pm 2.7 \times 10^{-6}$ gram/cm^3.

EXPERIMENTAL SETUP AND PROCEDURE

A 1-watt cw argon ion laser operating in the TEM_{00} mode at 5145 Å was used as the light source. An etalon in the laser cavity extended the coherence length to several meters to reduce the problems associated with conventional interferometric light sources in precisely matching object and reference beam optical path lengths. A spectrum analyzer was used for initially alining the etalon and periodic monitoring of the laser spectrum to maintain maximum fringe contrast. The laser was power tuned before each run for maximum output. A number 2 neutral density filter was used to reduce the output power to a safe level for system alinement. The maintenance and tuning of the laser was not difficult and required only a few minutes before a run. No special precautions were taken for vibration isolation of the laser.

All optical components except the laser, folding mirror, and streak camera were mounted on steel supports weighing 340 kilograms and supported on air cushions. The supports on each side of the test section were connected together. Laser beam directing, splitting, diverging, and filtering optics (Figs. 3 and 4) were positioned on a stable mount which was attached to the main support frame. The tapped hole pattern on the mount provided ease and stability in the initial setup as well as convenience in realinement when the system was moved to the different test sections.

The laser beam directing mirrors had 99% reflectivity at 5145 Å and were flat to $\lambda/8$ over a 5-mm aperture. This was more than adequate for the unexpanded 1-mm-diameter laser beam. The variable ratio beam splitter was interferometrically stable so that an adjustment of the reference-to-object beam intensity ratio required no realinement in the rest of the setup. This beam splitter was flat to $\lambda/10$ over a 1-mm aperture and had a light loss of about 10%. The 15-cm-diameter, f/8 collimating mirrors were parabolic to about $\lambda/20$ over the surface and had a reflectivity of about 80%. These mirrors could be tilted or translated by means of precision drive screws. The microscope objective-pinhole spatial filter mount consisted of a 25-micron pinhole movable in a plane perpendicular to the direction of propagation of the laser beam and a standard 10X microscope objective which could be translated along the beam direction. The 3.8-cm-thick test section windows were flat to about $\lambda/10$ over any 2 cm^2 area. These windows had an approximate 30-minute wedge in the y direction so that any interference fringes formed by multiple reflections within the windows themselves would be of such a high spatial frequency so as not to interfere with the low-frequency interference pattern used to measure the density.

Holograms were recorded using both Kodak 649F and the more sensitive Agfa 10E56 photographic plates. Since the hologram was made when steady-state conditions existed (prerun), the sensitivity of the photographic plates was not a problem and both types of plates worked equally well. It was found that holograms of excellent quality were possible without elaborate and time-consuming development procedures. For most of the runs, the holograms were bleached using either Kodak's chromium intensifier A solution or R-10 formula (7,8).

The bleached phase holograms were more efficient and resulted in brighter fringes.

A rotating camera and slit were used to record test data. Film transport speeds up to 48 meters/sec were possible with this camera. Kodak high-speed 2484 film was overdeveloped for 1.25 minutes at 35° C in Ethol 90 or in Kodak's D-19 to increase the sensitivity to about 3200 ASA. With this quick development procedure, the film record could be examined after about 6 minutes. The overdevelopment was necessary only if visual measurements of the fringe displacement were made rather than measurements with a microdensitometer.

The Pilot Model Expansion Tube was used to evaluate this technique. This facility (9) consists of a driver chamber, intermediate chamber, and acceleration chamber. A steel disphragm separates the driver and intermediate chambers and a mylar diaphragm separates the intermediate and acceleration chambers. The pressures in the chambers are adjusted to give the desired simulated environment. The bursting of the steel diaphragm causes a shock wave to propagate downstream which, in turn, bursts the mylar diaphragm. A new shock wave followed by the test gas then propagates downstream. Typical pressures used for this work were 2×10^7 newtons/meter^2 (2900 psia) of helium driver gas, 6.6×10^3 newtons/meter^2 (0.9 psia) of air in the intermediate chamber, and 38 newtons/meter^2 (5×10^{-3} psia) of air in the acceleration chamber. The tube had a square cross section of 70.5 cm^2. Test sections could be located at 0.9, 1.8, and 5 meters downstream of the secondary diaphragm. Typical interface and shock velocities for these tests were 4800 m/sec and 5800 m/sec, respectively.

The static, no-flow hologram was exposed with either atmospheric pressure or the prerun pressure in the test section. This was possible due to the long coherence length of the laser and because the object beam wave front was no different in either case so long as there were no density gradients in the test section. The variable-ratio beam splitter was adjusted so that the intensities of the object and reference beams were equal at the hologram. After an exposure of about 0.01 second, the hologram was developed using normal procedures and then bleached. The hologram was then replaced in its holder and the three-axes positioner adjusted to give a convenient spatial frequency and orientation of the fringes. The variable-ratio beam splitter was then adjusted so that the contrast of the fringe pattern was maximum. One static hologram usually gave acceptable results until the setup was moved to another test-section location or an adjustment was made in the optical setup.

The passage of the shock ionized gas by an upstream probe triggered the electronic shutter to open for about 15 milliseconds. This exposure prevented rewriting on the film during the 16.7 milliseconds for one revolution of the rotating drum. Since the disturbance of interest lasted only a few milliseconds, precise triggering was not needed. The 0.048-mm/μs camera writing speed and vertical slit width of 0.15 mm provided a time resolution of about 3 microseconds.

RESULTS AND DATA ANALYSIS

The fringe shifts were measured from the drum camera film strip (Fig. 5). For convenience, the fringe count was started on a perturbed fringe itself. A straight line parallel to the time axis was then drawn from the point where the fringe shift measurement was being made to the undisturbed fringe region on the film strip. The fringe shift was determined by counting the fringes which the straight line crossed and adding to this value the fraction of a fringe shift from the last fringe crossed (Fig. 6). The direction as well as magnitude of the fringe shift determines the density – the direction being dependent on the orientation of the recording camera.

If there are density reversals in the flow and hence fringe direction reversals (Fig. 5), a single fringe may be crossed more than once. For these cases the fringe shift can still be measured without ambiguity since the points where the straight line intersects the same fringe twice are points of equal phase shift from the undisturbed condition and hence are equal density points. (The fringe itself is not a line of constant density.)

The magnitude of the fringe shift is measured from a reference fringe where the density is known. For this application, the density in the expansion tube acceleration chamber was calculated using the perfect-gas law after measuring the pressure and temperature. A typical density in the acceleration chamber was approximately 0.45×10^{-6} grams/cm^3. For the typical initial facility parameters used in this study, a density ratio of 10 was expected across the shock wave. Therefore, the density across the shock was expected to increase to about 4.5×10^{-6} grams/cm^3. This change amounted to about 0.15 of a fringe shift and the fringes could easily be followed through the shock without misinterpreting the fringe number. Figure 7 is a typical plot of average density versus test section height at some time after the shock has passed the slit.

A simple method to visualize the flow is to superpose a film strip of the undisturbed fringes taken with no flow onto the film strip containing the disturbed fringes taken during flow. This superposition of film strips produces a Moiré fringe pattern (Fig. 8) where the Moiré fringes are lines of constant density. Care must be exercised in using the Moiré pattern to obtain quantitative density information when density reversals are expected, since the Moiré pattern is dependent only on the magnitude of the fringe shift, not the direction.

CONCLUSIONS

From the results of this study, it has been concluded that:

1. A real-time holographic interferometer can be applied to an aerodynamic facility with little more alinement difficulty than required for a

schlieren system and is suitable for routine facility operation.

2. The system can be used to measure the average density of high-velocity flows as a function of time.

3. The reference unperturbed fringes can be easily adjusted for the desired spatial frequency and orientation.

4. A time resolution of 3 microseconds is possible with this technique using a 0.5-watt argon laser and high-speed streak camera.

5. The technique is most applicable for measuring density variations in flow regions where the density gradient is not extreme.

REFERENCES

(1) John Winckler, "The Mach Interferometer Applied to Studying an Axially Symmetric Supersonic Air Jet," REV. SCI. INST., VOL. 19, NO. 5, pp. 307-322, May 1948.

(2) R. C. Jagota and D. J. Collins, "Finite Fringe Holographic Interferometry Applied to a Right Circular Cone at Angle of Attack," J. APPL. MECH., Dec. 1972.

(3) George Havener and Roger J. Radley, "Quantitative Measurements Using Dual Hologram Interferometry," ARL 72-0085, June 1972.

(4) Robert C. Spencer and Shiela A. T. Anthony, "Real-Time Holographic Moiré Patterns for Flow Visualization," APPL. OPTICS, VOL. 7, NO. 3, p. 561, March 1968.

(5) Howard M. Smith, "Principles of Holography," JOHN WILEY AND SONS, INC., 1969.

(6) Max Born and Emil Wolf, "Principles of Optics," PERGAMON PRESS, INC., 1959.

(7) J. H. Altman, "Pure Relief Images on Type 649-F Plates," APPL. OPTICS, VOL. 5, NO. 10, 1689-1690, Oct. 1966.

(8) W. T. Cathey, "Three-Dimensional Wavefront Reconstruction Using a Phase Hologram," J. OPT. SOC. AM., VOL. 55, NO. 4, p. 457, April 1965.

(9) Robert L. Trimpi, "A Preliminary Study of a New Device for Producing High-Enthalpy, Short-Duration Gas Flows," ADVANCES IN HYPERVELOCITY TECHNIQUES, ARTHUR M. KRILL, ED., PLENUM PRESS, pp. 425-451, 1962.

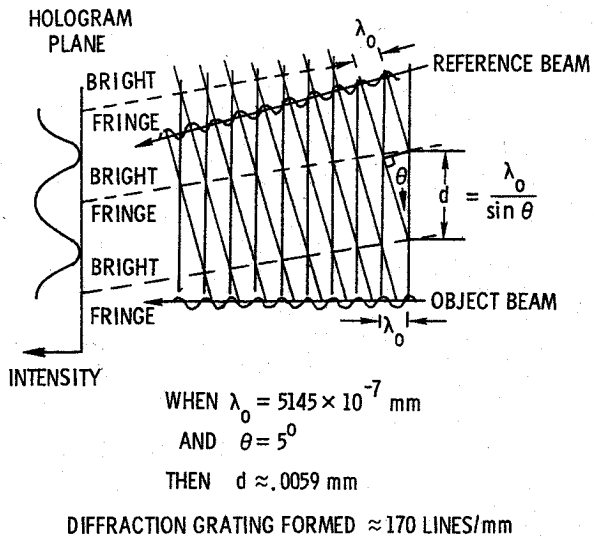

Figure 1. Formation of interference pattern recorded as hologram.

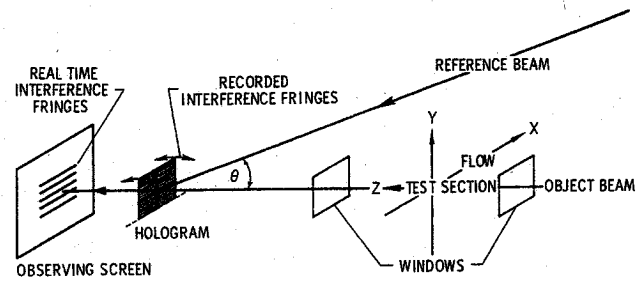

Figure 2. Formation of real-time fringes after hologram repositioned.

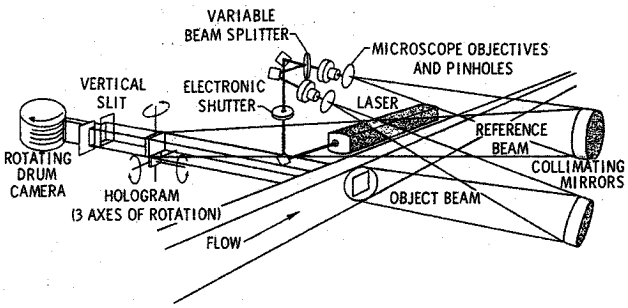

Figure 3. Sketch of setup.

Figure 4. Photograph of setup.

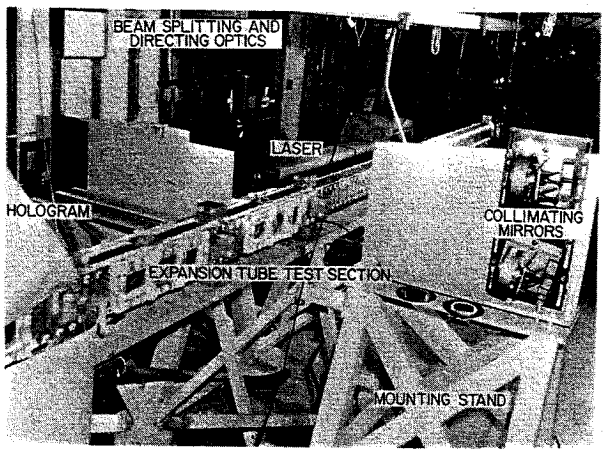

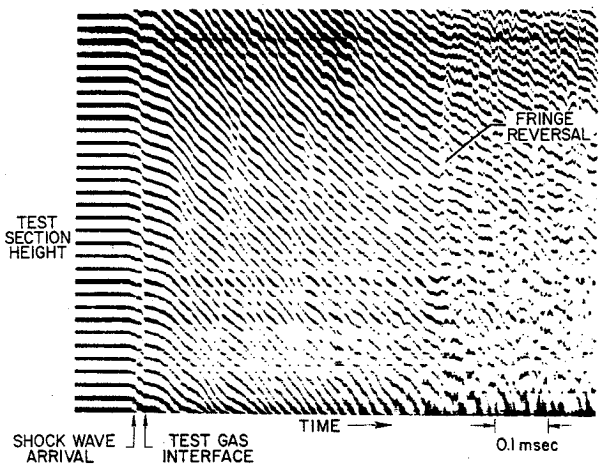

Figure 5. Typical interferogram.

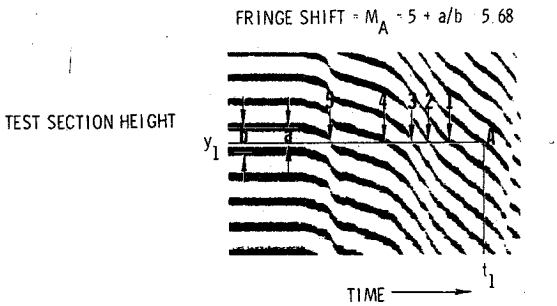

AVERAGE DENSITY AT A = $\rho_0 + (M_A \lambda_0)/(kl) = \rho_0 + 1.54 \times 10^{-4}$ g/cm^3

Figure 6. Procedure for calculating density at "A" on the interferogram.

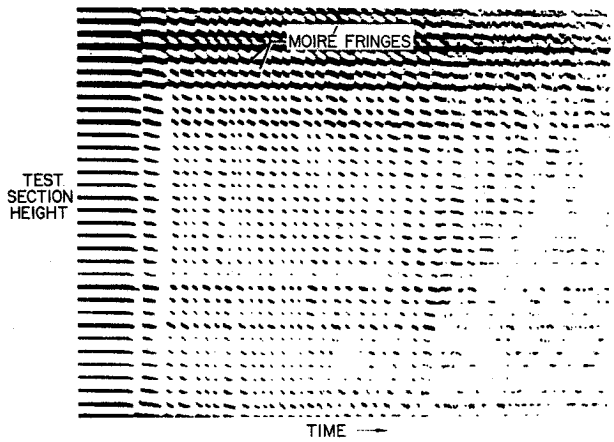

Figure 7. Plot of average density versus test-section height.

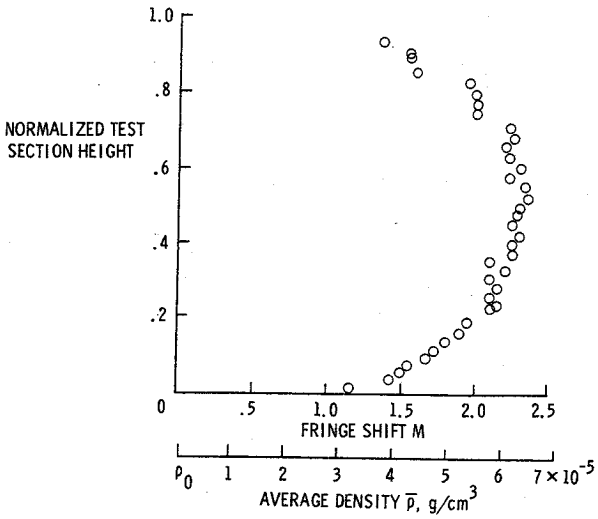

Figure 8. Moiré fringes obtained by superimposing disturbed and undisturbed fringe records.